Contents lists available at ScienceDirect

Materials Chemistry and Physics

journal homepage: www.elsevier.com/locate/matchemphys

Comparison of different reducing agents for the synthesis of mayenite electride C12A7:2e⁻ and a new photometric method to determine its electron density

Nils L. Kotschote [ID], Stefan G. Ebbinghaus [*] [ID]

Institut für Chemie, Martin-Luther-Universität Halle-Wittenberg, Kurt-Mothes-Straße 2, D-06120, Halle/Saale, Germany

HIGHLIGHTS

- With the reducing agents C, Ti, and Zr electrides with different electron densities ($Ca_{12}Al_{14}O_{33-x}(2e^-)_x$) were obtained.
- A new dichromate-based photometry was established as a simple, fast and accurate method to determine the electron contents.
- Compared to iodometric titration and conductivity measurements the photometry yields better reproducible results.

ARTICLE INFO

ABSTRACT

Discovered in 2003 the mayenite electride ($Ca_{12}Al_{14}O_{33-x}(2e^-)_x$) is the first electride being stable under ambient conditions. Different reaction conditions are known to result in samples with strongly deviating electron contents x. Various methods for determining x have been applied but have individual disadvantages. Therefore, a new alternative approach based on the reduction of dichromate and its photometric quantification is introduced and evaluated in this paper. For this, mayenite oxide was synthesised via classical solid-state synthesis and afterwards reduced by heating pellets embedded in the respective reducing agents under dynamic vacuum. Using carbon, titanium and zirconium as oxygen getters, different degrees of reduction were achieved. The electron densities of the obtained electrides were determined using iodometric titration, conductivity measurements and the new dichromate based photometry. Our results show that the latter method is feasible, robust and leads to well-reproducible, reliable values.

1. Introduction

Electrides are materials containing electrons as the smallest possible 'anions'. The first electrides were synthesised by dissolving alkali metals in liquid ammonia in 1908 [1] leading to 'solvated electrons' and later crown ethers were applied to stabilise the metal cations [2,3]. In 1986, the first crystal structure of an electride, $Cs^+(18C_6)_2\ e^-$, was published [4]. Later discovered electrides were also based on alkali metals stabilised with organic ligands [5–7]. All these electrides are both temperature unstable and moisture sensitive. In 2003 Hosono *et al.* reported on the first room-temperature stable electride synthesised by reducing $Ca_{12}Al_{14}O_{33}$ (C12A7, mayenite) with Ca metal [8]. Mayenite can be described as a positively charged antizeolithe-like framework with O^{2-} anions occupying 1/6 of the cages formed by the $[Ca_{12}Al_{14}O_{32}]^{2+}$

framework. These 'cage oxygen ions' are in fact part of disordered AlO_4-tetrahedra [9] and are replaced by electrons during the reduction process [10]. With increasing electron content a transition from insulating to semiconducting and finally to metallic conductivity occurs [11, 12]. Simultaneously, the colour changes from white/colourless to green and finally black [8] accompanied by an increase up to 0.02 Å of the lattice parameter *a* [13]. A complete replacement of cage oxide ions by electrons, *i.e.* formation of $Ca_{12}Al_{14}O_{32}(2e^-)$ corresponds to an electron density of $2.33 \times 10^{21}\ cm^{-3}$.

One of the most important analytic tasks for mayenite electrides is the determination of their electron densities. Different attempts have been described in literature. One possibility is electron paramagnetic resonance (EPR) [8,14–16]. The cage electrons lead to a Lorentzian-shape signal at g = 1.994, reflecting the F^+ like centres where

the electrons are located [8,17]. For the calculation of the electron density it is usually assumed that the electrons are unpaired and isolated and show a Curie paramagnetism [8,14]. However, at high electron densities antiparallel spin coupling occurs, resulting in too small EPR signals and also reduced magnetic moments found in *e.g.* SQUID investigations [18]. Therefore, EPR and magnetic measurements can only determine lower electron densities correctly.

Another method for determining the electron content are conductivity measurements [12,14,15,19–21]. The electron transport follows a 3D variable range hopping (VRH) mechanism for lower N_e values, *i.e.* log $\rho \propto T^{-1/4}$ [14,15,21]. With increasing electron density this conductivity changes to a metallic one [22–24]. Simultaneously, the resistivity at room temperature decreases by several orders of magnitude and therefore is a sensitive measure for the electron density. This in principle very straightforward method suffers from two drawbacks: First, it can only be used for dense ceramic samples or single crystals as the samples need to be contacted. Second, and more important, for a quantitative analysis a calibration with samples of known N_e is needed. Therefore, the electron densities of these reference samples must first be evaluated by another technique [16,25]. The second method that refers to electrical conductivity is the calculation of N_e using the Seebeck coefficient [8,24]. It was shown that the Seebeck coefficient has a linear dependence on log N_e at 300 K [8]. Yet, this method suffers from the same drawbacks, *i.e.* it relies on reference samples and only dense samples can be used.

An alternative possibility is the thermogravimetric analysis of the reoxidation of electrides to the parent oxide [13,22,26]. By this method, the electron contents can be determined without reference samples. Unfortunately, the full oxidation of the electride corresponds to a very small weight gain of only 1.17 %. Therefore, even small experimental errors (e.g. an insufficient buoyancy correction) can lead to false results. In addition, the (partial) incorporation of other oxygen species like O^-, O_2^{2-} or O_2^- can lead to increased weight gains [10,20,26–28]. Therefore, thermogravimetric measurements are prone to several potential errors.

Based on the change in colour, the idea of early works was to determine the electron density quantitatively with photometry, especially by optical reflection spectroscopy [8,14,17,19,29,30]. The incorporation of electrons in the mayenite framework leads to absorption peaks at 0.4 eV [30] and 2.8 eV [29]. The absorption at 0.4 eV results from an inter-cage electron transition between neighbouring cages and the one at 2.8 eV is caused by an intra-cage transition [19,21,25,29]. The exact position of the 2.8 eV peak shifts to lower energies with higher electron concentrations [13]. Other possible encaged anions are also distinguishable from the electride [17], *e.g.* oxide anions lead to a measurable absorption at 3.5 eV [31] and higher [32]. Recent work suggests that there are high discrepancies in the determination of low electron densities compared to other methods like iodometry, conductivity measurement or thermogravimetry, which show comparable values for different electron densities [22]. Therefore, optical reflection spectroscopy is only used for qualitative analyses in recent papers [33]. UV–Vis measurements in transmission geometry, on the other hand, show a strong dependence on microstructure effects for low N_e values whereas at high values an almost complete absorption due to the black colour of the samples occurs [34].

Another optical method to investigate electrides is Raman spectroscopy. Based on the Raman spectra, the cage anions can be distinguished as electrons, different oxygen species or various other anions [15, 35–37]. Varying electron densities result in significant changes in the spectra. At N_e values above 3×10^{20} cm^{-3} a prominent peak appears at 186 cm^{-1} originating from the cage electrons [15]. The peak intensity increases with the electron density. Additional changes like an increasing peak at 430 cm^{-1} and a decreasing peak at 560 cm^{-1} have been reported, too [15,38]. These features are attributed to changes of the Al–O bonds [15,18,36]. Yet, up to date no direct correlation between the peak intensities and the electron densities have been reported. Therefore, Raman spectroscopy cannot be applied for a quantification

but is rather used to identify samples as an electride or an oxide [38].

Alternatively, iodometry has been used to determine the degree of reduction. In this method, the electride is dissolved in hydrochloric acid in the presence of a defined excess quantity of I_2, which is partly reduced to I^-. The remaining I_2 is determined by titration with thiosulfate standard solution [22]. In contrast to other methods, iodometric titration does not need reference samples of known (or at least assumed) electron concentrations but provides absolute values. On the other hand, iodometry was found to very sensitivity to light and oxygen [39] and therefore might lead to erroneous results.

For these reasons, a new versatile and reliable method to directly (*i.e.* without reference samples) measure the electron content in mayenite electrides is required. We therefore established a photometric method based on the redox system $Cr_2O_7^{2-}/Cr^{3+}$ according to Eq. (1).

$$Cr_2O_7^{2-} + 14\,H^+ + 6e^- \rightarrow 2Cr^{3+} + 7H_2O \tag{1}$$
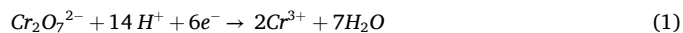
Dichromate is an established chemical for titrations and can be used as a titrimetric standard [40]. Compared to iodine solutions, dichromate solutions are very stable and have well-determined absorption spectra. Due to these characteristics they are also suitable for the calibration of photometers [41–43]. Changes in the concentration of dichromate upon reduction with electrides should be measurable and by using a defined excess of dichromate the absolute amount of electrons should be quantifiable.

In this work, a dichromate-based photometry for the direct determining of the electron density of mayenite electrides is evaluated in comparison with other methods and it is applied to mayenite electrides obtained with different reduction agents.

2. Experimental

2.1. Synthesis

Polycrystalline $Ca_{12}Al_{14}O_{33}$ was prepared via solid-state synthesis. 25.0905 g $CaCO_3$ (high purity, Solvay) and 15.0959 g α-Al_2O_3 (99.999 wt%, Yimintech) were mixed in the stoichiometric ratio of (nearly) 12:7 with isopropanol for 12 h in a planetary ball mill (Fritsch Pulverisette) with polyamide grinding bowl and balls. To prevent the formation of the C3A-phase ($Ca_3Al_2O_6$), a small excess of 1.25 mol % α-Al_2O_3 was used [9]. After milling, the mixture was dried and heated in an alumina crucible for 24 h at 1200 °C in air in a box furnace (Nabertherm HT04-17). The cooled obtained mayenite was wet ground with isopropanol for 12 h and dried.

The resulting powder was pressed into pellets of 16 mm diameter and weights of $\approx$2 g at 5 kN and sintered for 12 h at 1325 °C in air. For reduction, the sintered pellets were embedded in the reducing agent in alumina crucibles and heated in a tube furnace (ELITE TSH16/50/180) for 10 h at (nominally) 1420 °C (samples 1–6, Table 3). During heating, the tube was dynamically evacuated to $\approx$10^{-5} mbar. After the reaction temperature was reached, the tube was sealed with a ball valve to maintain a static vacuum, comparable to synthesis in sealed silica glass tubes. The furnace setpoint temperature of 1420 °C differs slightly from the temperature of the sample, which is roughly 5 °C below its melting point because a slight increase of 5 °C of the setpoint leads to melting of the samples. It should be noted that for the oxide mayenite different melting points have been reported in the range of 1392°C–1449 °C [44–48] and 1415 °C for mayenite electride [8]. After cooling down to room temperature pressures of $\approx$10^{-5} mbar for the reduction with Ti and Zr and $\approx$10^{-2} mbar for C were measured. The two samples Ti$_{1390}$ and Zr$_{1390}$ were synthesised accordingly except that the furnace set temperature was 1390 °C. The setup of the furnace and vacuum pump is shown in the Supplementary Fig. S1.

The surface of the resulting electride pellets were abraded. For analyses, half of each pellet was milled to powder in a zirconia grinding jar and grinding ball for 4 min with amplitude of 50 and 1 min with 70 in a

RETSCH MM 2000 swing mill.

2.2. Characterization

For powder X-ray diffraction (XRD) a Bruker D8-Advance diffractometer with Cu $K_{\alpha 1,2}$ radiation and a 1D silicon strip detector was used. XRD patterns in the angular range 15°–150° 2θ were used for Rietveld refinements performed with Fullprof (2022).

Four-probe conductivity measurements were performed in a Quantum Design Physical Property Measurement System (PPMS-9) at 300 K. For this, the second half of the electride pellets were cut into rods of approximately $1 \times 1 \times 10$ mm^3 (see Fig. 1) and contacted with silver paint (ACHESON 1415, PLANO). The DC current passing through the sample is automatically adjusted to yield the maximum resolution, but was limited to ≤ 1 mA. The resulting voltage drop is measured between two contacts on the top as shown in Fig. 1b. The resistivity is calculated by averaging two measurements with inverted polarity taking into account the geometry of the samples. The electron density was determined by linear fitting of the data from Kim et al. [16] on a double logarithmic scale (see supplemental).

For iodometry [22] ca. 14 mg of electride powder was weighed in a Schlenk vessel under Ar to prevent a potential oxidation of I$^-$ by oxygen. A well-defined mixture of 2 ml iodine solution (10^{-2} M) and 5 ml of hydrochloric acid (3×10^{-1} M) was added. After dissolving and reduction, the remaining iodine was titrated with a standard solution of thiosulfate (2×10^{-3} M) using starch as indicator. Reference measurements were done with the same amount of mayenite oxide. For each sample, the titration was repeated three times.

For determination of the electron density by the dichromate-based photometry, a 1.25 mmol l^{-1} solution of potassium dichromate was prepared by dissolving 367.73 mg potassium dichromate (p.A.) and 42 ml 37 % hydrochloric acid (analytic reagent grade, Fischer chemical) in 1 l deionized water. A chromium(III) solution (2.5 mmol l^{-1}) was made from 167.36 mg chromium(III)chloride hexahydrate (99.5 %, Alfa Aesar) and 10.5 ml 37 % hydrochloric acid (analytic reagent grade, Fischer chemical) in 250 ml deionized water. The five solutions used for calibration were prepared from mixtures of the dichromate and chromium(III) solution in varying amounts. Due to the carcinogenic and mutagenic effects of dichromate, appropriate safety precautions like gloves should be taken when handling this chemical.

For the determination of the electron contents 10.5 mg of each electride sample was dissolved in 4 ml of the acidic dichromate solution under magnetically stirring for 15 min. The reaction equation for the perfect electride is given in Eq. (2).

$$3\,(Ca_{12}Al_{14}O_{32}:2e) + Cr_2O_7^{2-} + 206\,H^+ \rightarrow 2\,Cr^{3+} + 103\,H_2O + 36\,Ca^{2+} + 42\,Al^{3+}$$

$$(2)$$
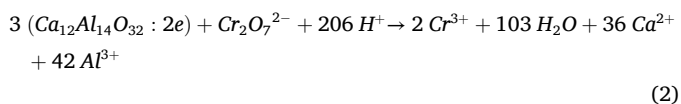
The absorption was measured at 440 nm in polystyrene cuvettes (10 mm optical path length, 3.5 ml volume) in a Cary 60 UV–Vis spectrophotometer (Agilent Technologies). The measurements were repeated three times. The concentration of dichromate was determined using the calibration curve mentioned above and shown in Fig. 5. This procedure was repeated three times for each sample and the electron density was determined as the average of these measurements.
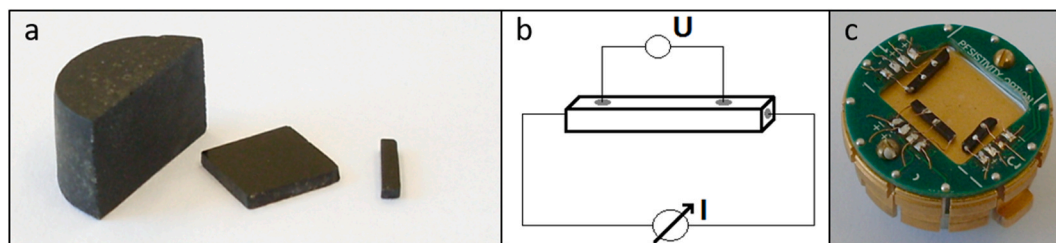
3. Results and discussion

3.1. Phase analysis of the synthesised electrides

Phase purity of the polycrystalline $Ca_{12}Al_{14}O_{33}$ starting oxide was checked by powder XRD (Fig. 2) and no impurity phases were detected. After reduction, the electride pellets had a sintered skin, which was abraded prior to the investigations. All electride pellets were black, whereas after grinding the colour of the resulting powders varied from green (carbon as reducing agent/oxygen getter) to brown (titanium) and finally black (zirconium) (Fig. 3). This already indicated strong difference in the electron densities [8]. The XRD pattern (Fig. 2) show no impurities apart from traces of $CaAl_2O_4$ (CA) identified from its main peak at 30.5°.

Lattice parameters were determined by Rietveld refinements (Fig. 4). The incorporation of electrons is known to cause an increase of the cubic lattice constant a [13,49]. The results listed in Table 1 clearly indicate that with increasing electron content (as derived from the changing colour) the value of a increases. Unfortunately, we found that this behaviour cannot be used to quantify the electron content, *i.e.* earlier investigations showed that samples with similar electron contents had different cell parameters.
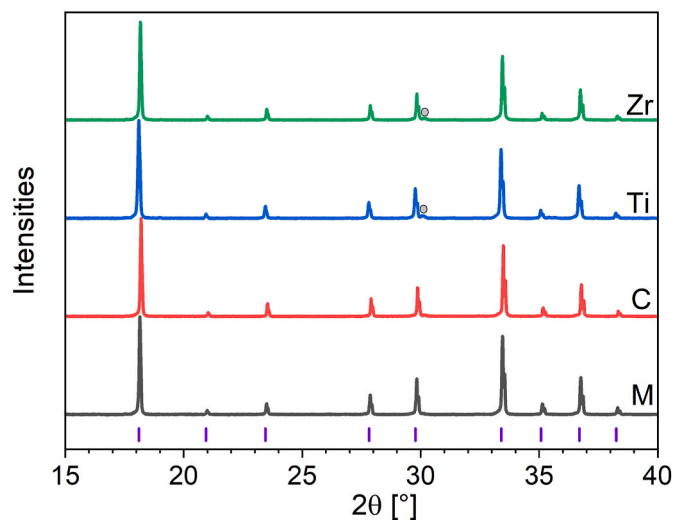
Fig. 2. Powder X-ray diffraction pattern of the polycrystalline oxide mayenite (M) and selected electride samples. The tick marks belong to the reference COD4308076. The small circle marks the main peak of the $CaAl_2O_4$ (CA).

Fig. 1. a: Preparation of the bars for conductivity measurements. b: scheme of the four-probe measurement set-up. c: photograph of three contacted electride samples on a PPMS-9 sample holder.
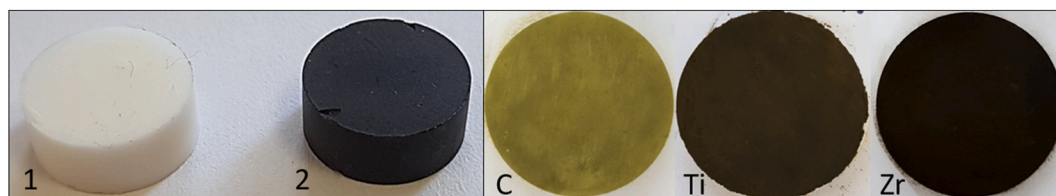
Fig. 3. Photographs a mayenite pellet before reduction (1) and an electride pellet (2). On the right powdered electride samples obtained from the reduction with carbon (sample no. 1), titanium (sample no. 5) and zirconium (sample no. 6) are shown.
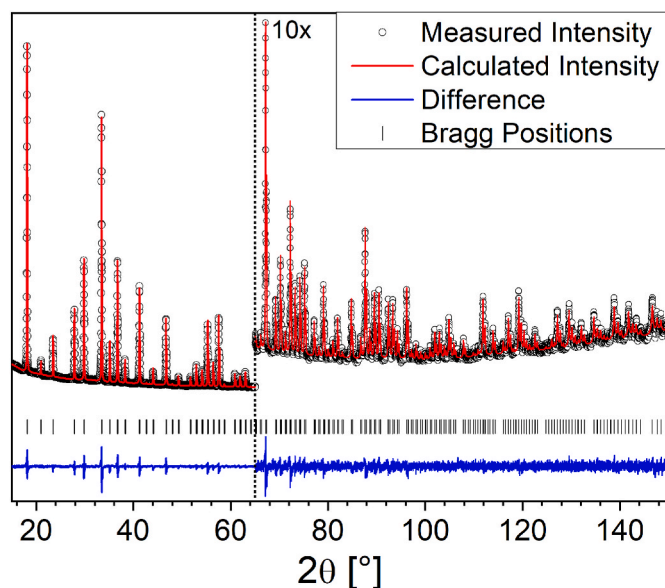
Fig. 4. Exemplary Rietveld refinement for an electride sample obtained from the reduction with carbon (sample 1).
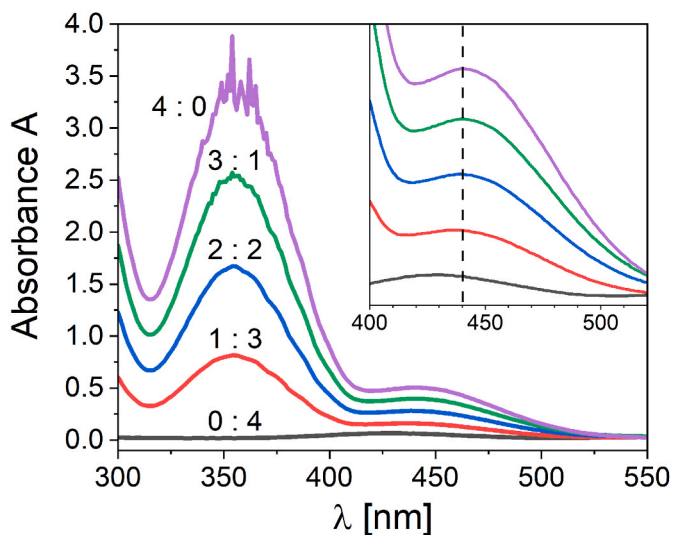
Fig. 5. UV–Vis spectra of the dichromate:Cr (III) reference solutions used for calibration of the photometry. The given values reflect the ratio of 1.25 mM dichromate and the 2.5 mM chromium-III solution with 10.5 mg of dissolved oxide mayenite. The wavelength of 440 nm used for concentration measurements is marked in the inset.

Table 1
Lattice parameters of the polycrystalline mayenite and the electride samples.

sample no.	reducing agent	Lattice parameter [Å]
Mayenite	–	11.9801(4)
1	C	11.9911(3)
2	C	11.9912(3)
3	C	11.9916(4)
4	C	11.9927(3)
5	Ti	11.9966(3)
6	Zr	11.9959(3)

3.2. Evaluation of the photometric measurement

Our photometric method is based on the different absorption spectra of $Cr_2O_7^{2-}$ and Cr^{3+} [42,50]. As the first step of the dichromate photometry, suitable values for the mass of the electride samples and the concentration of the dichromate solution were established by practicability considerations: First, repeated measurement should be possible without requiring too much of the sample, *i.e.* small masses for each measurement are desired. On the other hand, lower masses are more prone to weighing errors. The mass of 10.5 mg turned out to be most practicable. Based on the measurement of differences in absorption spectra the usage of a dichromate excess is advantageous. After several weeks, the concentration of the dichromate slightly decreases. To avoid errors based on this concentration change and to get a higher absorbance, the excess was chosen to be twice the stoichiometric ratio of the needed dichromate for the oxidation of 10.5 mg perfect electride, *i.e.* with two electrons per formula unit. Due to the high standard redox potential of 1.38 V for dichromate, it can be assumed that no other reduction reactions (in particular the reaction of H^+ to H_2 or Cr^{3+} to $Cr^{2+/0}$) will take place. As visible in Fig. 5, the dichromate solution shows two absorption peaks at 350 nm and 440 nm, respectively and usually the one at 350 nm is used for photometry [42,43]. To assure a good linear dependence according to the Lambert-Beer law the absorbance should be well below a value of 1.2 [51]. Using the 350 nm peak corresponds to a dichromate concentration below 350 µmol l^{-1}. As the required amount to oxidise 10 mg electride is ca. 2.5×10^{-3} mmol a total volume of ca. 14 ml would be required. Because only 3.5 ml of solution is needed for the photometric measurement, this would result in a large volume of toxic waste. For this reason, the concentration measurements of the dichromate solution was done using the 440 nm peak, which has already been chosen for photometry in a previous work [42]. A reasonable absorbance of 0.5 at this wavelength is obtained with a dichromate solution of 1.25 mmol l^{-1}. In addition, the wide plateau of this peak is also advantageous for preventing errors caused by slight peak shifting.

Calibration of the photometry was done with five solutions of varying ratios $Cr_2O_7^{2-}:Cr^{3+}$ (4:0; 3:1; 2:2; 1:3 and 0:4). In each solution, 10.5 mg of oxide mayenite was dissolved to take into account possible matrix effects. UV–Vis spectra for the solutions are shown in Fig. 5. The measured absorbance is plotted as a function of the dichromate concentration as shown Fig. 6. The behaviour can well be described using a linear fit, which in the following was used to calculate the remaining dichromate concentration after reduction of the electride samples.
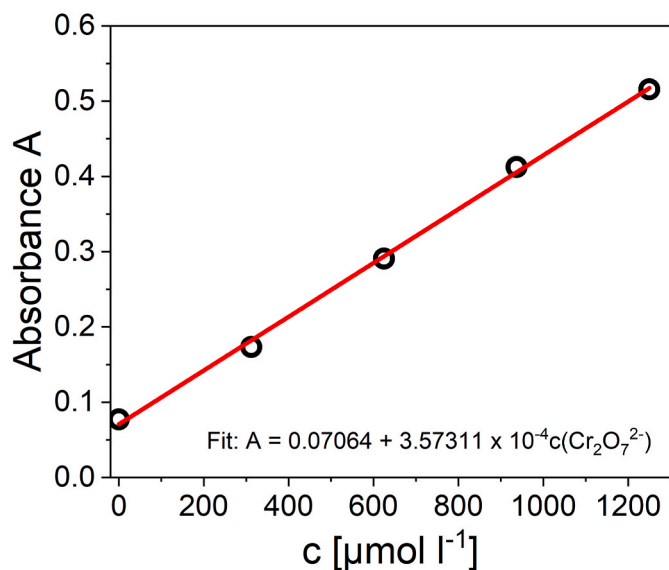
Fig. 6. Absorbance at 440 nm of the dichromate solutions used for calibration and its linear fit.

The degree of reduction x, which indicates the replacement of caged oxygen with electrons (where 0 corresponds to the pure oxide and 1 to two electrons per formula unit) was calculated according to Eq (3). c_0 and c_1 are the dichromate concentrations before and after reduction of the electride, V is the applied solution volume, m the sample mass, and z is the equivalent number. Its value z = 3 results from the six electrons required for the dichromate reduction (1) and the two electrons per formula unit in the ideal mayenite electride. M is the molar mass, which slightly depends on x. As the difference of M for the oxide and the electride is only about 1 %, the average can used in the calculations without generating a considerable error. The electron density is calculated according to equation (3).

$$x = (c_0 - c_1) \bullet V \bullet m \bullet M \bullet z \tag{3}$$

$$N_e = 2.33 \bullet 10^{21} cm^{-3} \bullet x \tag{4}$$

Table 2 lists the obtained values from five independent measurements of three samples with varying electron densities. These samples were reduced with titanium (1390 °C), zirconium (1390 °C) and zirconium (1420 °C). Details of the results are listed in the Supplementary

Table 2

Repeated determination of the difference in concentration, the calculated electron content x according to the formula $Ca_{12}Al_{14}O_{33-x}(2e^-)_x$ and the electron density (N_e) for selected electride samples Ti_{1390} (reduced with titanium for 10 h at 1390 °C), Zr_{1390} (reduced with zirconium for 10 h at 1390 °C), and Zr_{1420} (reduced with zirconium for 10 h at 1420 °C) by the dichromate based photometry including standard deviations.

Ti_{1390}	1	2	3	4	5	Ø
c_0-c_1 [µoll⁻¹]	152.0	152.3	161.4	160.0	160.9	157(5)
x	0.244	0.245	0.258	0.257	0.255	0.251(6)
N_e [10^{21} cm⁻³]	0.57	0.57	0.60	0.60	0.59	0.59(2)
					Ø Coefficient of variation of x and N_e: 2.4 %	
Zr_{1390}	1	2	3	4	5	Ø
c_0-c_1 [µoll⁻¹]	237.3	256.9	231.6	248.0	237.0	242(9)
x	0.376	0.396	0.375	0.386	0.377	0.382(8)
N_e [10^{21} cm⁻³]	0.88	0.92	0.87	0.90	0.88	0.89(2)
					Ø Coefficient of variation of x and N_e: 2.1 %	
Zr_{1420}	1	2	3	4	5	Ø
c_0-c_1 [µoll⁻¹]	287.5	309.2	302.2	327.2	297.0	304(13)
x	0.475	0.481	0.475	0.457	0.471	0.471(8)
N_e [10^{21} cm⁻³]	1.11	1.12	1.11	1.07	1.10	1.10(2)
					Ø Coefficient of variation of x and N_e: 1.3 %	

Table S1. The different samples were chosen because they contain deviating electron densities [35,36,52,53]. The average coefficient of variation of x and N_e accounts to only 1.3 % for a high electron density (x ≈ 0.5) and 2.4 % for a lower density (x ≈ 0.25) indicating a well reproducible determination of varying electron densities.

The dichromate based photometry is a new way to determine the electron content of mayenite electrides. The time required for each sample is only about 30 min and half of the time involves dissolving the sample. In addition, only a small sample amount of ca. 10 mg is required.

Our investigations show that the accuracy slightly increases for higher electron densities. Measurements of very low electron contents with x < 0.1 show a higher variance of the electron content.

One disadvantage of our photometric method is the use of carcinogenic dichromate, which requires appropriate safety precautions during handling. Before disposal the dichromate should be reduced to the less harmful Cr^{3+} e.g. with sodium thiosulfate.

3.3. Comparison of the different methods for determining the electron density

The results obtained from the dichromate based photometry were compared with the iodometric titration and conductivity measurement. The obtained values are listed in Table 3 and the experimental data is given in the Supplementary Table S1. The results for four different electride samples reduced with carbon under identical conditions yield almost the same electron densities of ca. 0.48×10^{-3} when determined by electrical conductivity and photometry. This on the one hand indicates that the two methods give comparable results and on the other hand, that the reduction with carbon reproducibly yields electrides with similar electron densities. In contrast, the results of the iodometric titration differ between 0.14 and 0.47×10^{-3} for the four samples and therefore are apparently less reliable. The observed deviations are probably due to the high sensitivity of the iodometry to light and O_2, causing oxidation of iodine. Additionally, the pH value has a strong impact on the results: For well-reproducible iodometry, the pH range should be slightly acidic to neutral [40], whereas a pH value of ca. 0.5 has to be applied for a fast, quantitative dissolving of the electride in order to prevent side reactions [22]. This rather low pH value might be a reason for the deviating results.

Two additional electride samples were obtained with titanium and zirconium as oxygen getters. In the case of Ti the conductivity measurements yielded a lower electron density than the iodometry and photometry (0.65 *vs.* 0.75×10^{21} cm⁻³, respectively), whereas for the sample reduced with Zr all three methods yield very similar values of 1.1×10^{21} cm⁻³, corresponding to a degree of reduction x ≈ 0.5. The increase of electron density is in accordance with the Ellingham diagrams of the three reducing agents, which predict a decreasing oxygen partial pressure in the order C, Ti, and Zr [54].

Table 3

Electron densities (N_e) determined by electrical conductivity measurements, iodometric titration and dichromate-based photometry for samples reduced with different agents. The values of the photometry are the average of two measurements.

sample no.	reducing agent	N_e [10^{21}cm⁻³]		
		conductivity	iodometry	photometry
1	C	0.47	0.47	0.47
2	C	0.49	0.14	0.49
3	C	0.49	0.23	0.49
4	C	0.47	0.19	0.47
5	Ti	0.65	0.76	0.77
6	Zr	1.10	1.09	1.10

4. Conclusion

In this work, mayenite electrides with deviating electron densities were synthesised by reaction with various reducing agents. The reactions were carried out in vacuum (ca. 5×10^{-5} mbar) in an alumina tube that was separated from the vacuum pump after reaching the final reaction temperature. The obtained electrides were used to establish a new dichromate-based photometry method for determining the electron densities. In previous publications, several methods have been described. Among them, the iodometric titration and resistivity measurements are most often used. The former suffers from the fact that the results depend on the pH of the solution and the time between dissolving and titration. The resistivity measurements are prone to contact problems *e.g.* due to an oxidation of the sample surface and the fact that it requires reference samples with known electron densities. In this paper, it was shown that the dichromate-based photometry allows a fast, reliable and reproducible determination of the electron densities of electride samples with varying N_e values without the need of references.

CRediT authorship contribution statement

Nils L. Kotschote: Writing – original draft, Methodology, Investigation. **Stefan G. Ebbinghaus:** Writing – review & editing, Project administration.

Funding

Declaration of competing interest

The authors declare that they have no known competing financial interests or personal relationships that could have appeared to influence the work reported in this paper.

Appendix A. Supplementary data

Supplementary data to this article can be found online at https://doi.org/10.1016/j.matchemphys.2025.130513.

Data availability

Data will be made available on request.

References

[1] C.A. Kraus, Solutions of metals in non-metallic solvents; IV. 1 material effects accompanying the passage of an electrical current through solutions of metals in liquid ammonia. Migration experiments, J. Am. Chem. Soc. 30 (1908) 1323–1344, https://doi.org/10.1021/ja01951a001.

[2] J.L. Dye, J.M. Ceraso, M. Lok, B.L. Barnett, F.J. Tehan, Crystalline salt of the sodium anion (Na-), J. Am. Chem. Soc. 96 (1974) 608–609, https://doi.org/10.1021/ja00809a060.

[3] C.J. Pedersen, Cyclic polyethers and their complexes with metal salts, J. Am. Chem. Soc. 89 (1967) 2495–2496, https://doi.org/10.1021/ja00986a052.

[4] S.B. Dawes, D.L. Ward, R.H. Huang, J.L. Dye, First electride crystal structure, J. Am. Chem. Soc. 108 (1986) 3534–3535, https://doi.org/10.1021/ja00272a073.

[5] R.H. Huang, M.J. Wagner, D.J. Gilbert, K.A. Reidy-Cedergren, D.L. Ward, M. K. Faber, J.L. Dye, Structure and Properties of Li$^+$ (Cryptand [2.1.1])e$^-$ - an Electride with a 1D "Spin-Ladder-like" Cavity-Channel Geometry, J. Am. Chem. Soc. 119 (1997) 3765–3772, https://doi.org/10.1021/ja9640760.

[6] M.J. Wagner, R.H. Huang, J.L. Eglin, J.L. Dye, An electride with a large six-electron ring, Nature 368 (1994) 726–729, https://doi.org/10.1038/368726a0.

[7] D.L. Ward, R.H. Huang, J.L. Dye, Structures of alkalides and electrides. I. Structure of potassium cryptand[2.2.2] electride, Acta Crystallogr C Cryst Struct Commun 44 (1988) 1374–1376, https://doi.org/10.1107/S0108270188002847.

[8] S. Matsuishi, Y. Toda, M. Miyakawa, K. Hayashi, T. Kamiya, M. Hirano, I. Tanaka, H. Hosono, High-density electron anions in a nanoporous single crystal: Ca$_{24}$Al$_{28}$O$_{64}^{4+}$(4e$^-$), Science 301 (2003) 626–629, https://doi.org/10.1126/science.1083842.

[9] S.G. Ebbinghaus, H. Krause, F. Syrowatka, Floating zone growth of large and defect-free Ca$_{12}$Al$_{14}$O$_{33}$ single crystals, Cryst. Growth Des. 13 (2013) 2990–2994, https://doi.org/10.1021/cg400406t.

[10] L. Palacios, A.G. de La Torre, S. Bruque, J.L. García-Muñoz, S. García-Granda, D. Sheptyakov, M.A.G. Aranda, Crystal structures and in-situ formation study of mayenite electrides, Inorg. Chem. 46 (2007) 4167–4176, https://doi.org/10.1021/ic0700497.

[11] M. Miyakawa, S.W. Kim, M. Hirano, Y. Kohama, H. Kawaji, T. Atake, H. Ikegami, K. Kono, H. Hosono, Superconductivity in an inorganic electride 12CaOx7Al$_2$O$_3$:e$^-$, J. Am. Chem. Soc. 129 (2007) 7270–7271, https://doi.org/10.1021/ja0724644.

[12] S.W. Kim, S. Matsuishi, T. Nomura, Y. Kubota, M. Takata, K. Hayashi, T. Kamiya, M. Hirano, H. Hosono, Metallic state in a lime-alumina compound with nanoporous structure, Nano Lett. 7 (2007) 1138–1143, https://doi.org/10.1021/nl062717b.

[13] S. Matsuishi, T. Nomura, M. Hirano, K. Kodama, S. Shamoto, H. Hosono, Direct Synthesis of Powdery Inorganic Electride [Ca$_{24}$Al$_{28}$O$_{64}$]$^{4+}$(e$^-$)$_4$ and Determination of Oxygen Stoichiometry, Chem. Mater. 21 (2009) 2589–2591, https://doi.org/10.1021/cm9007987.

[14] S. Matsuishi, S.W. Kim, T. Kamiya, M. Hirano, H. Hosono, Localized and delocalized electrons in room-temperature stable electride [Ca$_{24}$Al$_{28}$O$_{64}$]$^{4+}$(O^{2-})$_{2-x}$(e$^-$)$_{2x}$ analysis of optical reflectance spectra, J. Phys. Chem. C 112 (2008) 4753–4760, https://doi.org/10.1021/jp711631j.

[15] S.W. Kim, T. Shimoyama, H. Hosono, Solvated electrons in high-temperature melts and glasses of the room-temperature stable electride Ca$_{24}$Al$_{28}$O$_{64}^{4+}$·4e$^-$, Science 333 (2011) 71–74, https://doi.org/10.1126/science.1204394.

[16] S. Kim, M. Miyakawa, K. Hayashi, T. Sakai, M. Hirano, H. Hosono, Simple and efficient fabrication of room temperature stable electride: melt-solidification and glass ceramics, J. Am. Chem. Soc. 127 (2005) 1370–1371, https://doi.org/10.1021/ja043990n.

[17] K. Hayashi, S. Matsuishi, T. Kamiya, M. Hirano, H. Hosono, Light-induced conversion of an insulating refractory oxide into a persistent electronic conductor, Nature 419 (2002) 462–465, https://doi.org/10.1038/nature01053.

[18] F. Li, X. Zhang, H. Liu, J. Zhao, Y. Xiao, Q. Feng, J. Zhang, In situ synthesis of [Ca$_{24}$Al$_{28}$O$_{64}$]$^{4+}$ (4e$^-$) electride ceramic from C12A7 + C3A mixture precursor, J. Am. Ceram. Soc. (2018), https://doi.org/10.1111/jace.16103.

[19] T. Kamiya, S. Aiba, M. Miyakawa, K. Nomura, S. Matsuishi, K. Hayashi, K. Ueda, M. Hirano, H. Hosono, Field-Induced current modulation in nanoporous semiconductor, electron-doped 12CaO·7Al$_2$O$_3$, Chem. Mater. 17 (2005) 6311–6316, https://doi.org/10.1021/cm051904s.

[20] Y. Toda, Y. Kubota, M. Hirano, H. Hirayama, H. Hosono, Surface of room-temperature-stable electride Ca$_{24}$Al$_{28}$O$_{64}^{4+}$(e$^-$)$_4$: preparation and its characterization by atomic-resolution scanning tunneling microscopy, ACS Nano 5 (2011) 1907–1914, https://doi.org/10.1021/nn102839k.

[21] S.-W. Kim, K. Hayashi, M. Hirano, H. Hosono, I. Tanaka, Electron carrier generation in a refractory oxide 12CaO·7Al$_2$O$_3$ by heating in reducing atmosphere: conversion from an insulator to a persistent conductor, J. Am. Ceram. Soc. 89 (2006) 3294–3298, https://doi.org/10.1111/j.1551-2916.2006.01213.x.

[22] T. Yoshizumi, S. Matsuishi, S.-W. Kim, H. Hosono, K. Hayashi, Iodometric determination of electrons incorporated into cages in 12CaO·7Al$_2$O$_3$ crystals, J. Phys. Chem. C 114 (2010) 15354–15357, https://doi.org/10.1021/jp1054364.

[23] P.V. Sushko, A.L. Shluger, M. Hirano, H. Hosono, From insulator to electride: a theoretical model of nanoporous oxide 12CaO·7Al$_2$O$_3$, J. Am. Chem. Soc. 129 (2007) 942–951, https://doi.org/10.1021/ja066177w.

[24] S.W. Kim, R. Tarumi, H. Iwasaki, H. Ohta, M. Hirano, H. Hosono, Thermal conductivity and Seebeck coefficient of 12CaO·7Al$_2$O$_3$ electride with a cage structure, Phys. Rev. B 80 (2009), https://doi.org/10.1103/PhysRevB.80.075201.

[25] S.-W. Kim, S. Matsuishi, M. Miyakawa, K. Hayashi, M. Hirano, H. Hosono, Fabrication of room temperature-stable 12CaO·7Al$_2$O$_3$ electride: a review, J. Mater. Sci. Mater. Electron. 18 (2007) 5–14, https://doi.org/10.1007/s10854-007-9183-y.

[26] O. Trofymluk, Y. Toda, H. Hosono, A. Navrotsky, Energetics of formation and oxidation of microporous calcium aluminates: a new class of electrides and ionic

conductors, Chem. Mater. 17 (2005) 5574–5579, https://doi.org/10.1021/cm051662w.

[27] Y. Dong, H. Hosono, K. Hayashi, Formation and quantification of peroxide anions in nanocages of 12CaO·7Al2O3, RSC Adv. 3 (2013) 18311, https://doi.org/10.1039/c3ra42521e.

[28] K. Hayashi, M. Hirano, S. Matsuishi, H. Hosono, Microporous crystal 12CaO·7Al$_2$O$_3$ Encaging Abundant O$^-$ Radicals, J. Am. Chem. Soc. 124 (2002) 738–739, https://doi.org/10.1021/ja016112n.

[29] P.V. Sushko, A.L. Shluger, K. Hayashi, M. Hirano, H. Hosono, Hopping and optical absorption of electrons in nano-porous crystal 12CaO·7Al$_2$O$_3$, Thin Solid Films 445 (2003) 161–167, https://doi.org/10.1016/S0040-6090(03)01156-8.

[30] Y. Toda, H. Yanagi, E. Ikenaga, J.J. Kim, M. Kobata, S. Ueda, T. Kamiya, M. Hirano, K. Kobayashi, H. Hosono, Work function of a room-temperature, stable electride [Ca$_{24}$Al$_{28}$O$_{64}$]$^{4+}$(e$^-$)$_4$, Adv. Mater. 19 (2007) 3564–3569, https://doi.org/10.1002/adma.200700663.

[31] S. Kanbara, M. Kitano, Y. Inoue, T. Yokoyama, M. Hara, H. Hosono, Mechanism switching of ammonia synthesis over Ru-loaded electride catalyst at metal-insulator transition, J. Am. Chem. Soc. 137 (2015) 14517–14524, https://doi.org/10.1021/jacs.5b10145.

[32] D. Jiang, Z. Zhao, S. Mu, V. Phaneuf, J. Tong, Simple and efficient fabrication of mayenite electrides from a solution-derived precursor, Inorg. Chem. 56 (2017) 11702–11709, https://doi.org/10.1021/acs.inorgchem.7b01655.

[33] D. Jiang, Z. Zhao, S. Mu, H. Qian, J. Tong, Facile and massive aluminothermic synthesis of mayenite electrides from cost-effective oxide and metal precursors, Inorg. Chem. 58 (2019) 960–967, https://doi.org/10.1021/acs.inorgchem.8b03116.

[34] R.P.S.M. Lobo, N. Bontemps, M.I. Bertoni, T.O. Mason, K.R. Poeppelmeier, A. J. Freeman, M.S. Park, J.E. Medvedeva, Optical conductivity of mayenite: from insulator to metal, J. Phys. Chem. C 119 (2015) 8849–8856, https://doi.org/10.1021/acs.jpcc.5b00736.

[35] J.-P. Eufinger, A. Schmidt, M. Lerch, J. Janek, Novel anion conductors– conductivity, thermodynamic stability and hydration of anion-substituted mayenite-type cage compounds C12A7:X (X = O, OH, Cl, F, CN, S, N), Phys. Chem. Chem. Phys. 17 (2015) 6844–6857, https://doi.org/10.1039/c4cp05442c.

[36] C. Phrompet, C. Sriwong, P. Srepusharawoot, S. Maensiri, P. Chindaprasirt, C. Ruttanapun, Effect of free oxygen radical anions and free electrons in a Ca$_{12}$Al$_{14}$O$_{33}$ cement structure on its optical, electronic and antibacterial properties, Heliyon 5 (2019) e01808, https://doi.org/10.1016/j.heliyon.2019.e01808.

[37] V. Lalan, S. Ganesanpotti, The smallest anions, induced porosity and graphene interfaces in C12A7:e$^-$ electrides: a paradigm shift in electromagnetic absorbers and shielding materials, J. Mater. Chem. C 10 (2022) 969–982, https://doi.org/10.1039/d1tc03762e.

[38] M. Reitemeyer, D. Zschätzsch, K. Holste, L. Chen, P. Klar, Applicability of Electride Materials for Hollow Cathodes, 2019.

[39] W. Zou, K. Khan, X. Zhao, C. Zhu, J. Huang, J. Li, Y. Yang, W. Song, Direct fabrication of C12A7 electride target and room temperature deposition of thin films with low work function, Mater. Res. Express 4 (2017) 36408, https://doi.org/10.1088/2053-1591/aa63c7.

[40] G. Jander, Massanalyse: Titrationen mit chemischen und physikalischen Indikationen, De Gruyter, Berlin/Boston, 2017.

[41] F.C. Conceição, E.M. Silva, J.F.S. Gomes, P.P. Borges, Characterization of potassium dichromate solutions for spectrophotometercalibration, J. Phys.: Conf. Ser. 975 (2018) 12028, https://doi.org/10.1088/1742-6596/975/1/012028.

[42] R.W. Burke, R. Mavrodineanu, Acidic potassium dichromate solutions as ultraviolet absorbance standards, J. Res. Natl. Bur. Stand. A Phys. Chem. 80A (1976) 631–636, https://doi.org/10.6028/jres.080A.062.

[43] A. Malinauskas, R. Holze, An in situ UV-Vis spectroelectrochemical investigation of the dichromate reduction at a polyaniline-modified electrode, Ber. Bunsen Ges. Phys. Chem. 102 (1998) 982–984, https://doi.org/10.1002/bbpc.19981020713.

[44] J.A. Imlach, Phase equilibria in the system CaO-Al$_2$O$_3$-TiO$_2$, Trans. Br. Ceram. Soc. 67 (1968) 581.

[45] G.A. Rankin, The ternary system CaO-Al$_2$O$_3$-SiO$_2$ with optical study by F. E. Wright, Am. J. Sci. s4-39 (1915) 1–79, https://doi.org/10.2475/ajs.s4-39.229.1.

[46] R.W. Nurse, The 12CaO·7Al$_2$O$_3$ phase in the CaO-Al$_2$O$_3$ system, Trans. Br. Ceram. Soc. 64 (1965) 323.

[47] A.K. Chatterjee, G.I. Zhmoidin, The phase equilibrium diagram of the system CaO-Al$_2$O$_3$-CaF$_2$, J. Mater. Sci. 7 (1972) 93–97, https://doi.org/10.1007/BF00549555.

[48] B. Hallstedl, Assessment of the CaO-Al$_2$O$_3$ system, J. Am. Ceram. Soc. 73 (1990) 15–23, https://doi.org/10.1111/j.1151-2916.1990.tb05083.x.

[49] J.R. Salasin, S.E.A. Schwerzler, R. Mukherjee, D.J. Keffer, K.E. Sickafus, C.J. Rawn, Direct Formation and structural characterization of electride C12A7, Materials 12 (2018), https://doi.org/10.3390/ma12010084.

[50] P.J. Elving, B. Zemel, Absorption in the ultraviolet and visible regions of chloroaquochromium(III) ions in acid media, J. Am. Chem. Soc. 79 (1957) 1281–1285, https://doi.org/10.1021/ja01563a006.

[51] P. Wörfel, M. Bitzer, U. Claus H. Felber, M. Hübel, B. Vollenweider, Analytische Methoden, Springer Basel AG, Basel, 1990.

[52] A.A. Rybak, I.D. Yushkov, N.A. Nikolaev, A.V. Kapishnikov, A.M. Volodin, G. K. Krivyakin, G.N. Kamaev, P.V. Geydt, Electrophysical Properties of Polycrystalline C12A7:e$^-$ Electride, Electronics 11 (2022) 668, https://doi.org/10.3390/electronics11040668.

[53] U. Khopongpaiboon, W. Jarernboon, V. Amornkitbamrung, B.N. Lampang, S. Sinthupinyo, P. Chindaprasirt, Effects of added carbon black on synthesis and characterization of calcium aluminate electride, in: The Second Materials Research Society of Thailand International Conference, AIP Publishing, Pattaya, Thailand, 2020 30001.

[54] M.J. Balart, J.B. Patel, F. Gao, Z. Fan, Grain refinement of deoxidized copper, Metall. Mater. Trans. 47 (2016) 4988–5011, https://doi.org/10.1007/s11661-016-3671-8.